Chain and Structural Dynamics in Melts of Sphere-Forming Diblock Copolymers

Anshul Chawla, Frank S. Bates, Kevin D. Dorfman,* and David C. Morse*

Department of Chemical Engineering and Materials Science, University of Minnesota – Twin Cities, 421 Washington Ave. SE, Minneapolis, MN 55455, USA

E-mail: dorfman@umn.edu; morse012@umn.edu

Abstract

Melts of asymmetric sphere-forming diblock copolymers form a dense liquid of micelles at temperatures above the order-disorder transition (ODT) temperature and below a critical micelle temperature (CMT), above which micelles dissolve. Molecular dynamics simulations were used to study how tracer diffusivity, the rate of chain exchange between micelles, and the rate of structural relaxation change with increasing degree of segregation or decreasing temperature in this state. Results for tracer diffusion and chain exchange are consistent with experimental results, and confirm that diffusion in well-segregated systems occurs via hops of chains between neighboring micelles. A structural relaxation time τ_{s} is obtained from decay of the dynamic structure factor $S(q^*, t)$ at the peak wavenumber q^*. The time τ_{s} increases dramatically with increasing degree of segregation, reaching values near the ODT of order 10^2 times the homopolymer Rouse time, with larger increases for systems with lower invariant degrees of polymerization. A theoretical prediction of the micelle lifetime, based on a model of stepwise micelle dissociation, yields an estimated lifetime of order $10^3\tau_s$ near the ODT, indicating that micelle birth and death may occur too slowly to be observed in these simulations. The relationship to experimental evidence is discussed.

Introduction

When a complex fluid is perturbed from equilibrium, equilibrium is restored through a variety of relaxation processes. For example, liquids of long homopolymers relax via relaxation of polymer conformations. Disordered materials that contain self-assembled micelles or other supramolecular aggregates relax much more slowly via processes that generally involve changes in both the positions and the number of such aggregates. In the present study, we use large-scale molecular dynamics (MD) simulations of a coarse-grained polymer model to study a variety of dynamical processes that occur in melts of compositionally asymmetric AB copolymers that form a disordered fluid of spherical micelles, with the goal of providing an understanding of the remarkably slow kinetics in these systems.[1–6]

Diblock copolymers in selective solvents tend to form micelles or other aggregates, much like small-molecule surfactants. Highly asymmetric AB diblock copolymers with a minority B block immersed in a solvent that favors contact with A tend to form spherical micelles with a B-rich core. Relaxation in a dense fluid of such micelles involves several dynamical processes with disparate relaxation times. The fastest processes involve local relaxation of chain conformations within micelles, which can occur over times comparable to the relaxation times observed in homopolymer melts. Longer times are required for exchange of molecules between micelles, due to the free energy cost of temporarily extracting the core block of a copolymer from a micelle. Long relaxation times are also expected for processes that rearrange the positions of micelles within a dense liquid, which is essential to the relaxation of stress that is measured in linear rheological experiments. Processes that change the number of micelles and the average micelle aggregation number may require even longer relaxation times, due to the existence of particularly large barriers to micelle creation and destruction, whether these processes occur by stepwise association and dissociation or by fission and fusion.[7–15] While substantial attention has been focused on characterizing this entire range of processes in micellar block copolymer solutions,[15] somewhat less work has been done on analogous problems in neat melts of compositionally asymmetric diblock copolymers.[2,6,16–18]

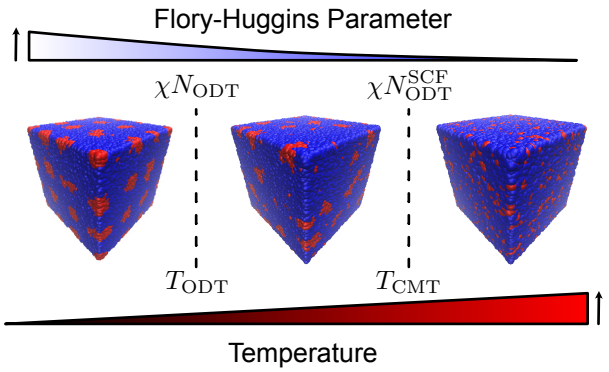

Figure 1: Structural changes of a compositionally asymmetric diblock copolymer melt as a function of temperature or, equivalently, as a function of the segregation strength χN. T_{ODT} and T_{CMT} are the order-disorder temperature and the critical micelle temperature, respectively. χN_{ODT} is the segregation strength at the true order-disorder transition temperature. $\chi N_{\mathrm{ODT}}^{\mathrm{SCF}}$ is the order-disorder transition predicted by self-consistent field theory.

One-component melts of sphere-forming diblock copolymers pass through three different structural states with increasing temperature or, equivalently, decreasing values of the product χN of the Flory-Huggins χ-parameter and degree of polymerization N. At sufficiently low temperatures or high χN, micelles formed by neat diblock copolymer melts pack on a lattice (Figure 1). Most systems form a body-centered cubic (BCC) lattice,[19] and a small region of close-packing is sometimes observed near the order-disorder transition (ODT).[20–22] Conformationally asymmetric systems with statistical segment lengths $b_{\mathrm{B}} > b_{\mathrm{A}}$, however, also form Frank-Kasper phases,[23] with σ and A15 formed at equilibrium[24–28] and the C14 and C15 Laves phases accessible through thermal processing.[4,5,29] As such a system is heated through the ODT temperature T_{ODT}, crystalline order is disrupted and the Bragg peaks observed in small-angle x-ray scattering (SAXS) in the ordered state are converted to the broad peak characteristic of a disordered micellar liquid.[30] Further heating causes a shift in the peak wavenumber q^* as the number of micelles changes,[2,6,31] followed by disappearance of micelles at the critical micelle temperature (CMT).

Equilibrium properties of diblock copolymer melts exhibit a universal dependence on the parameters that control behavior in self-consistent field theory (SCFT) and the invariant degree of polymerization $\overline{N}$. Self-consistent field predictions for diblock copolymer with

monomers of equal statistical segment length b depend on the minority block volume fraction f and the product χN. The invariant degree of polymerization for such a system is given by $\overline{N} = N(cb^3)^2$, where c is the concentration of monomers.[32] Theory and simulation suggest that the CMT occurs at a value of χN very close to the ODT value predicted by SCFT,[31,33–35] and that the ODT occurs at a higher value of χN that increases with decreasing $\overline{N}$. The width of the range of values of χN between the ODT and CMT in which a micellar liquid exists thus increases with decreasing $\overline{N}$. The width of this range is expected to vanish in the limit $\overline{N} \to \infty$, in which SCFT becomes exact, and in which the CMT and ODT coincide. Most experiments are, however, performed on systems with $\overline{N} \approx 10^2 - 10^4$,[36] in which the disordered micellar state persists over a sizable temperature range. Notably, systems that have been observed to form Frank-Kasper phases have tended to have rather low values of $\overline{N}$ and thus possess substantial disordered micelle regimes proximate to their ODTs. The increase in the value of χN at the ODT with decreasing $\overline{N}$ is relevant to our understanding of their dynamical behavior near the ODT, because systems with greater values of χN exhibit stronger segregation, and correspondingly longer relaxation times for all of the relevant dynamical processes in the disordered phase near the ODT.

Our interest in modeling the relaxation of the particle-forming diblock polymers is motivated in part by experimental evidence of anomalously long relaxation times observed in experiments as micellar-forming systems crystallize and melt. It has been known for over two decades that formation of a BCC crystal can take several days, and some systems may not crystallize at all.[1] A particularly notable example of the slow ordering of BCC was observed in experiments of Cavicchi and Lodge.[2] After first annealing either a poly(isoprene)-*b*-poly(styrene) (PI-PS) or poly(ethylene-*alt*-propylene-*b*-dimethylsiloxane (PEP-PDMS) system for several months to form BCC, the sample was then heated through T_{ODT}, with the anticipated disordering. Subsequent cooling below the ODT restored the BCC ordering, but at a larger primary peak wavenumber q^* than the initially annealed sample. Moreover, this higher q^* only returned to the annealed value after 100 hrs for the PI-PS sample, and failed

to do so for the PEP-PDMS system after 2 months. Remarkably, the time scale for diffusion over the unit cell in the latter system is only 10 s,[18] two orders of magnitude smaller than the annealing time and thus indicating that chain diffusion is not the rate limiting factor.[2]

Diblock copolymer melts that form Frank-Kasper phases and their related quasicrystals, which possess much more intricate unit cells when compared to BCC, exhibit even more remarkable dynamical behavior. The most salient examples are the thermal processing of poly(isoprene)-*b*-poly(lactide) (PI-PLA) melts.[3–5] When this system with minority block volume fraction $f_{\mathrm{PI}} = 0.15$ is cooled directly from the disordered state, it first forms BCC and then σ upon further cooling. Rapid cooling of the same polymer in liquid N_2 and subsequent reheating can instead yield a C14 Laves phase.[4] Remarkably, these systems appear to retain memory of their crystal structure even after a crystal is destroyed by heating through the ODT; the value of peak wavenumber q^* obtained from SAXS from the disordered phase after melting C14 differs by 15% from that obtained after melting a BCC crystal in the same system, and this difference was observed to persist for at least 30 min.[5] Moreover, C14 re-emerges after slow cooling of a disordered phase that was created by melting C14 back through the ODT.[5] Similar memory effects were also observed[5] with a cylinder-forming PI-PLA system ($f_{\mathrm{PI}} = 0.2$), which produces C15 after thermal processing.[4]

The experiments of Kim *et al.*[5] have thus demonstrated that non-equilibrium values of q^* can persist in the disordered phases for surprisingly long times, of order 10^3 seconds or more. Notably, these experiments were performed on systems of relatively low viscosity, for which the terminal rheological relaxation time appears to be less than one second.[37] This observation indicates that the mechanism by which q^* relaxes toward its equilibrium value must be distinct from, and much slower than, the process by which stress relaxes. Kim *et al.*[5] have hypothesized that micellar liquids at temperatures near the ODT might be able to relax stress via comparatively rapid re-arrangements in micelle positions, but that changes in q^* may be controlled by much slower processes that can change the micelle number concentration by creating or destroy entire micelles.

Patel *et al.*[6] have studied dynamics in disordered micellar diblock copolymer melts by comparing measurements of linear viscoelastic moduli to results of x-ray photon correlation spectroscopy (XPCS) experiments. These authors studied an asymmetric styrene-isoprene (SI) copolymer at temperatures slightly above T_{ODT}, in a system that forms a hexagonal phase at $T < T_{\mathrm{ODT}}$. Patel *et al.*[6] compared values of a structural relaxation time τ_{struc} that characterizes the decay of the X-ray intensity-intensity autocorrelation function $g_2(q,t)$ at a wavenumber q equal to the peak wavenumber q^* to the terminal rheological relaxation time τ_{tr} obtained from measurements of linear viscoelastic moduli. Strikingly, these authors obtained values of τ_{struc} that are 1-2 orders of magnitude greater than τ_{tr}. Like the experiments of Kim *et al.*,[5] these experiments thus demonstrated the existence of a structural relaxation time as detected by a scattering experiment that is significantly larger than τ_{tr}, though the disparity appears to be much less extreme than that observed in the experiments of Kim *et al.*[5] Comparison of these experiments is complicated by fact that different properties of the scattering signal were observed (i.e., relaxation of q^* vs. an intensity autocorrelation function), which may be sensitive to different types of structural relaxation.

The relationship between rheology and dynamic scattering has also been explored in a prior simulation study of disordered symmetric diblock copolymers by Ghasimakhbari and Morse.[38] In that work, MD simulations were used to measure both the stress relaxation modulus $G(t)$ and the dynamic structure factor $S(q,t)$. Near the lamellar-disorder transition, the terminal rheological relaxation time τ_{tr} was found to be very similar to a structural relaxation time τ_{s} inferred from the decay of $S(q^*,t)$ at the peak wavenumber. In fact, it was shown there[38] that the behavior of $G(t)$ could be rather accurately predicted by using the measured behavior of $S(q,t)$ as an input to the Fredrickson-Larson (FL) theory[39] of the effect of composition fluctuations on linear viscoelasticity, while adding a Rouse-like contribution to $G(t)$ to the contribution arising from composition fluctuations that is predicted by the FL theory.

In this work, we use molecular simulation in attempt to quantify some of the dynamical

phenomena underlying observations of sphere-forming melts, using well calibrated simulation models that have been shown to yield universal equilibrium behavior.[36,40] Simulations and experiments have complementary strengths and weaknesses. The strengths of simulations include the ability to measure quantities that are not easily accessible in experiments, the freedom to vary χN over wide ranges without encountering experimental constraints such as thermal degradation, and the ease with which one can vary $\overline{N}$ independently of χN. The limitations of simulations studies arise primarily from the need to study relatively small systems over simulation times much less than corresponding times accessible in experiments.

Simulation Method

The methodology of the simulations reported here closely follows that of our previous work[34,35] on analysis of equilibrium properties of sphere-forming systems. All results reported here are obtained from MD simulations of coarse-grained models of highly asymmetric AB copolymers with a soft non-bonded interaction and a harmonic bond potential. All potential energy parameters correspond to those of models referred to in earlier work[40] as models S1 and S2. These are models in which a parameter that controls the strength of repulsion between A and B beads can be adjusted to vary the effective χ parameter, while holding all other model parameters constant, and for which the relationship between χ and this adjustable parameter is known from prior work. The two systems considered both have $N = 64$ beads per chain and a volume fraction of $f_{\mathrm{B}} = 1/8$, or 8 beads in the minority B block, but have different invariant degrees of polymerization $\overline{N} = 960$ (model S1) and $\overline{N} = 3820$ (model S2). We sometimes refer to these two systems by the labels S1-64 and S2-64. Simulations of disordered phase for each model are performed over a range of χ from $\chi = 0$ (i.e., homopolymer melt) up to values for which an ordered state is stable. Simulations of the ordered phase are performed using an artificially initialized BCC crystal, in which the number of molecules is chosen so as to create a unit cell size that corresponds to an estimate

of the equilibrium value at each value of χN, with a 3 x 3 x 3 array of BCC unit cells (54 micelles), as described in previous work.[34,35] At conditions near the ODT, resulting systems contained roughly 6000 molecules for model S1-64 and 9000 molecules for model S2-64, which were simulated for 1-3 $\times 10^8$ MD steps (exact values are given in the supplemental information for Ref. 35). Further details of the simulation methodology are provided in the Supporting Information of this article and in previous related work.[34,35]

Chain Dynamics: Diffusion and Exchange

In this section, we characterize dynamics of individual chains by measuring tracer diffusivities and rates of exchange of molecules between micelles. To characterize diffusion, we measure the average mean-squared displacement

$$g(t) = \langle |\mathbf{R}(\tau + t) - \mathbf{R}(\tau)|^2 \rangle$$

of the center-of-mass $\mathbf{R}(t)$ as a function of time separation t and fit the behavior at long times to the expected linear behavior $g(t) = 6Dt$ for a polymer with diffusivity D. Results have been measured for both models of interest here over a range of values of χN in both disordered and ordered phases. Examples of resulting data for $g(t)$ are provided in supporting information (SI), Figure S1.

Figure 2 summarizes the resulting values for D as a function of the segregation strength χN_{B} calculated using the minority block degree of polymerization N_{B}.[16,18] The diffusivities are made dimensionless by dividing them by the diffusivity D_0 obtained in a system with $\chi = 0$ or, equivalently, by the tracer diffusivity of homopolymers with the same degree of polymerization.

Measured diffusivities for both models are nearly independent of χN_{B} at values less than the value $(\chi N_{\mathrm{B}})_{\mathrm{ODT}}^{\mathrm{SCF}}$ at which SCFT predicts an order-disorder transition, and decrease rapidly with increasing χN_{B} at higher values. Previous simulation work has shown that

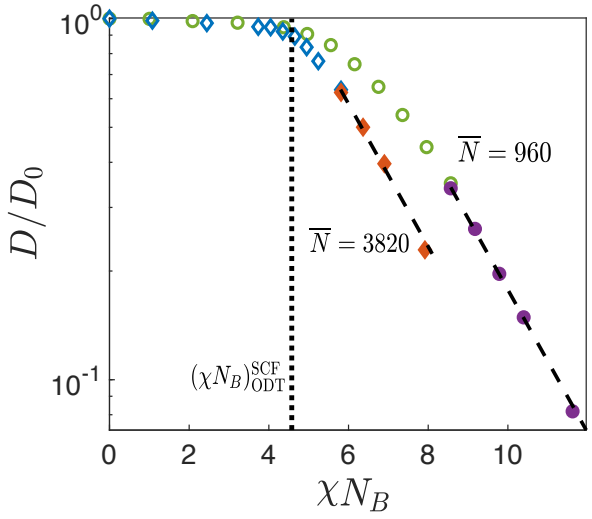

Figure 2: Tracer diffusivity of a single chain D normalized by the diffusivity of a homopolymer with the same chain length as a function of the product χN_{B}, where N_{B} is degree of polymerization of the core block. Circles and diamonds denote the diffusivity for simulations having $\overline{N} = 960$ and 3820 respectively. Open symbols represent results obtained in the disordered phase and closed symbols represent those obtained in an ordered BCC phase. The vertical dotted line is the prediction of the ODT from SCFT. The dashed lines are regression of the ordered state data to Eq. 1. For $\overline{N} = 960$, $D/D_0 = 16.83\exp[-0.4552(\chi N_{\mathrm{B}})]$ with a correlation coefficient of $R^2 = 0.9994$, and for $\overline{N} = 3820$, $D/D_0 = 8.914\exp[-0.4552(\chi N_{\mathrm{B}})]$ with $R^2 = 0.9947$.

$(\chi N_{\mathrm{B}})^{\mathrm{SCF}}_{\mathrm{ODT}}$ approximately corresponds to the CMT, above which micelles appear.[34,35] The segregation of copolymers into micelles clearly has a profound affect on diffusivity. Crystallization of micelles onto a lattice seems, however, to have no discernible affect; for both values of $\overline{N}$, we find no significant difference between values of D in the ordered and disordered phases at values of χN_{B} for which both phases remain stable over the course of a simulation. This observation is consistent with the experimental observations of Cavicchi and Lodge,[18] who also found that D is continuous across the ODT.

In more strongly segregated systems, or higher values of χN_{B}, D is well described by an approximately exponential function of χN_{B} of the form

$$\frac{D}{D_0} \sim \exp(-A\chi N_{\mathrm{B}}) \quad , \tag{1}$$

where A is a dimensionless $O(1)$ prefactor, as found in prior experimental work.[2,16,18] Fitting

of results of simulation of the ordered phase to Eq. 1 yields the fits shown by dashed lines in Figure 2, with a coefficient of $A \approx 0.45$ for both models. This value is roughly consistent with the value of A obtained in the BCC phase for the high molecular weight PEP-PDMS system studied by Cavicchi and Lodge,[18] but substantially less than the value $A \approx 1.2$ used to fit the experimental data for BCC-forming poly(styrene)-*b*-poly(2-vinylpyridine) (PS-P2VP).[2,16] The higher value of $\overline{N} = 3820$ simulated here is comparable to that of the PEP-PDMS 30-4 system studied by Cavicchi and Lodge,[18] for which $\overline{N} = 3770$. Hindered diffusion with behavior consistent with Eq. (1) has also been observed previously in Langevin simulations of individual chains diffusing in a static potential field that approximates the BCC structure.[17] It is gratifying to instead see behavior consistent with that found in experiments emerge here from direct many-chain simulations of a model in which micelles can form spontaneously. One important difference between our simulations and experimental systems, however, is the fact that these simulations use soft pair interactions that allow polymers to pass through each other, and thus exhibit unentangled Rouse-like dynamics, while different experimental systems may be entangled to greater or lesser degrees.[2]

We characterize the exchange of polymers between micelles by measuring the average number $n_L(t)$ of molecules that are in a particular micelle at any time τ that remain in the same micelle at a later time $\tau + t$. The identification of micelles, and of which molecules belong to which micelles, is performed using a cluster analysis that was described in our previous work.[34,35] We have performed this analysis only in the BCC ordered phase, which allows for the use of somewhat simplified rules to identify corresponding clusters at different times. Let $\tau_{\rm ex}$ denote the average time required to expel any specific polymer from within a micelle, or the lifetime of a polymer within a micelle. We identify $\tau_{\rm ex}$ by fitting data for $n_L(t)$ to the functional form

$$n_L(t) = Q \exp\left(-\frac{t}{\tau_{\rm ex}}\right) + c \quad , \tag{2}$$

in which Q is the average micelle aggregation number for a given value of $\overline{N}$ and χN, and c is a small constant.

We use a functional form in Eq. (2) that allows $n_L(t)$ to approach a small nonzero value $n_L(t) \to c$ in the limit $t \to \infty$, rather than assuming that $n_L(t) \to 0$ in this limit, to account for the fact that these simulations are carried out on a finite system of micelles with periodic boundary conditions. In such a system, there is a small but nonzero probability of a polymer returning to the same micelle even after an infinite delay. This argument predicts a value of $c = Q/n_{\rm m}$ where $n_{\rm m} = 54$ is the number of micelles in a system with 27 BCC unit cells. The value of c has been adjusted to fit the data, which yields fitted values of c that are similar to this prediction, but usually 10-30% larger.

In what follows, we non-dimensionalize values of $\tau_{\rm ex}$ by a characteristic homopolymer conformational relaxation time[38]

$$\tau_0 \equiv \frac{\zeta N^2 b^2}{6\pi^2 k_{\rm B} T} \quad , \tag{3}$$

in which $\zeta = k_{\rm B}T/(ND_0)$, where D_0 is the measured homopolymer diffusivity for the model of interest, $k_{\rm B}$ is Boltzmann's constant, and T is absolute temperature. This is the prediction of the Rouse model for the terminal relaxation time of the end-to-end vector calculated using bead friction coefficient ζ that is inferred from the homopolymer diffusivity.

Figure 3 shows both an example of our analysis of $n_L(t)$ and a summary of resulting values for $\tau_{\rm ex}$ in the BCC phase, normalized by τ_0. The inset of Figure 3 provides representative examples of results for $n_L(t)$ for $\overline{N} = 960$ at several values for χN, in which fits to Eq. (2) are shown by dashed lines. Corresponding results for $n_L(t)$ for $\overline{N} = 3820$ are provided in SI, Figure S2. The main plot in Figure 3 provides the resulting values of $\tau_{\rm ex}$ as a function of χN, shown as solid colored symbols connected by lines. Results for $\overline{N} = 3820$ and $\overline{N} = 960$ appear in different ranges of values of χN to accommodate the increase in $(\chi N)_{\rm ODT}$ with decreasing $\overline{N}$.

In a melt of strongly segregated micelles, diffusion might be expected to occur primarily via rare events in which a molecule is expelled from one micelle, diffuses through the A-rich

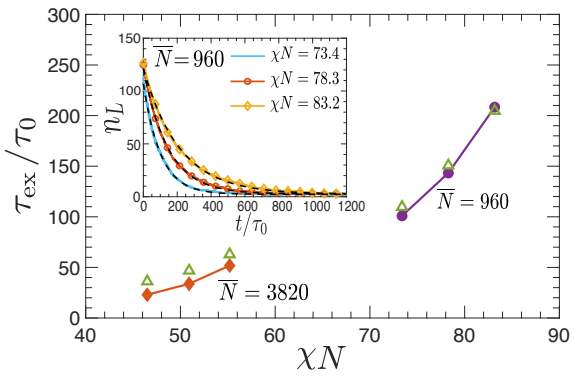

Figure 3: Main plot: Normalized chain exchange time τ_{ex}/τ_0 vs. segregation strength χN in simulations of ordered BCC phases, where τ_0 is the homopolymer Rouse relaxation time. Solid diamonds and circles indicate measured values of τ_{ex} for $\overline{N} = 3820$ and $\overline{N} = 960$, respectively. Open triangles show values of τ_{ex} that are inferred from values of the tracer diffusivity D by assuming that chains hop between nearest-neighbor micelles. Inset: Examples of data for the average number of polymers in a particular micelle, $n_L(t)$, vs. normalized delay time t/τ_0 that was fit to obtain measured values of τ_{ex}. Dashed lines show fits to Eq. (2).

region, and is absorbed into a neighboring micelle. To test the validity of this picture, we have considered a simple model in which each molecule can hop randomly from its current micelle to a micelle which is a nearest neighbor on a BCC lattice, with an average time τ_{ex} between such hops, while assuming a Markov process in which subsequent hops occur in statistically independent directions. This model gives a diffusivity $D = r^2/\tau_{ex}$, in which $r = \sqrt{3}a/2$ is the distance between nearest neighbors in a BCC lattice with a cubic lattice spacing a.

To test the validity of this simple nearest-neighbor hopping model for diffusivity, we have computed the value of τ_{ex} that would be inferred from the value of the tracer diffusivity D (as determined by measuring mean-squared displacements) while assuming the validity of this model. Values of τ_{ex} that were inferred from the diffusivity are shown as open triangles in the main plot of Figure 3, while measured values obtained from the time-dependence of $n_L(t)$ are shown as solid symbols. Agreement between measured and inferred values of τ_{ex} is excellent for the systems with $\overline{N} = 960$ (S1-64) for which the data was taken at higher values of χN (i.e., in more strongly segregated systems), and still reasonably good for $\overline{N} =$

3820 (S2-64). This agreement indicates that diffusion in the ordered phase is well described to a first approximation by such a hopping process, particularly at higher values of χN. Given that diffusivity appears to be unaffected by the appearance of order, we infer that the diffusivity in the disordered micelle regime is also dominated by hopping between micelles at conditions near the ODT. In systems with the higher value of $\overline{N} = 3820$, and lower values of χN, the inferred values of $\tau_{\rm ex}$ are slightly greater than the measured values, indicating that the measured diffusivity is greater than predicted by this model. This is consistent with the existence of a small contribution to D by some other mechanism, such as, *e.g.*, hopping to next-nearest neighbors on the lattice. As χN decreases further, and the fraction of free chains that remain outside of micelles increases, the physical picture underlying our model is unlikely to remain valid at conditions sufficiently near the CMT. This hopping picture is clearly inappropriate for states with $\chi N < (\chi N)_{\rm CMT}$, in which there are no micelles.

Structural Dynamics: Dynamic Structure Factor

In a dense liquid of micelles, the dynamic structure factor provides information about collective structural re-arrangements involving entire micelles. The dynamical structure factor $S(\mathbf{q}, t)$ for a diblock copolymer is defined as an ensemble average[41]

$$S(\mathbf{q}, t) = \frac{1}{V}\langle \hat{\psi}^*(\mathbf{q}, t)\hat{\psi}(\mathbf{q}, 0)\rangle \quad , \tag{4}$$

where V is the simulation volume and $\hat{\psi}(\mathbf{q}, t)$ is the spatial Fourier transform of the composition field $\psi(\mathbf{r}, t) \equiv [c_A(\mathbf{r}, t) - c_B(\mathbf{r}, t)]/2$, in which $c_i(\mathbf{r}, t)$ denotes the instantaneous concentration of monomers of type i at time t. Additional details on the computation of $S(\mathbf{q}, t)$ are provided in the Supporting Information. At $t = 0$, $S(\mathbf{q}, 0)$ reduces to the static structure factor measured by elastic small angle x-ray and neutron scattering. The rate of relaxation of $S(\mathbf{q}, t)$ in an isotropic liquid depends on wavenumber $q = |\mathbf{q}|$, and is known to be slowest for values of q nearest the wavenumber q^* at which the static structure factor

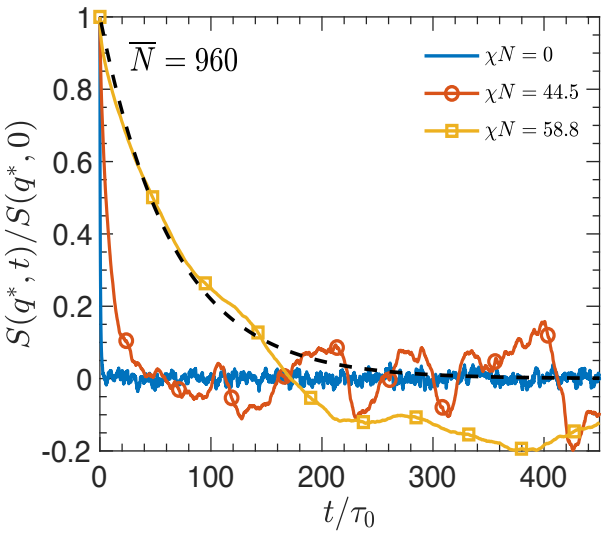

Figure 4: Normalized dynamical structure factor at the peak wavenumber $S(q^*,t)/S(q^*,0)$ *vs.* the normalized time t/τ_0, where τ_0 is the homopolymer Rouse relaxation time, for simulations with $\bar{N} = 960$ and three values of χN. Circle and square markers are used to help distinguish between the different curves and are shown every 2000 data points. The black dashed line is an example of exponential fit to the initial decay shown for $\chi N = 58.8$.

is maximum. The relaxation time of $S(q,t)$ for $q \simeq q^*$ is thus expected to yield a terminal relaxation time for structural re-arrangements in a micellar liquid.

Figure 4 provides several examples of the normalized dynamical structure factor $S(q^*,t)$ in the disordered phase for $\overline{N} = 960$ at several values of χN; similar data for $\overline{N} = 3820$ are provided in SI, Figure S3. To obtain a structural relaxation time, we fit the early time behavior of $S(q^*,t)$ to an exponential decay. As the relaxation time increases with increasing χN, our results for $S(q^*,t)$ become increasingly noisy, making it difficult for us to characterize the final decay of this function within a feasible computational time at conditions near the ODT. Our data quality is, however, sufficient to allow us to estimate the time constant for the initial decay of $S(q^*,t)$ to a factor of 3-5 times less than the initial value $S(q^*,0)$. In what follows, we use τ_s to denote the time constant extracted by fitting this initial decay of $S(q^*,t)$ to an exponential.

Figure 5 summarizes our results for structural relaxation times. For the homogeneous state, the structural relaxation time is smaller than the self-diffusion time by a factor of three.

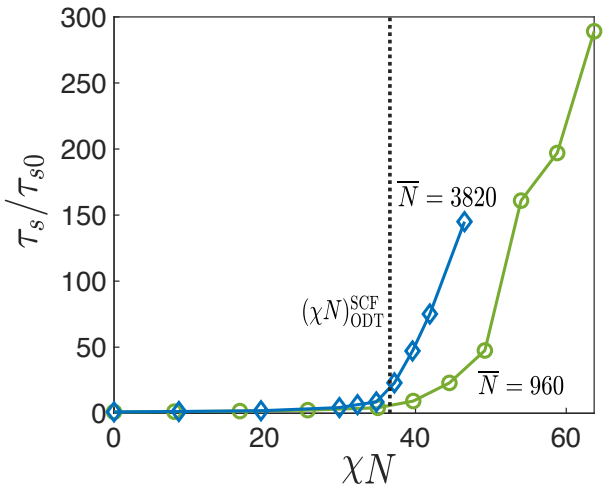

Figure 5: Structural relaxation time $\tau_{\rm s}$ for simulations with $\bar{N} = 960$ and 3820 normalized by the homopolymers structural relaxation time τ_{s0} (i.e., the value of τ_s at $\chi N = 0$)). We find that $\tau_{s0} = 0.334\tau_0$ for $\overline{N} = 960$ and $\tau_{s0} = 0.3158\tau_0$ for $\overline{N} = 3820$. Green circles and blue diamonds correspond to $\overline{N} = 960$ and 3820, respectively. The dotted vertical line shows the SCFT prediction for χN at the ODT.

When micelles begin to appear at $\chi N \simeq \chi N_{\rm ODT}^{\rm SCF}$, the structural relaxation time increases sharply, with the rate of increase being faster for the larger $\overline{N}$. Eventually, the curves in Figure 5 will be cut off by the ODT and the system should crystallize, as observed previously for lamellae-forming systems.[38] As a result, the structural relaxation time for the smaller $\overline{N}$ near its ODT is larger than that for the larger $\overline{N}$ at its ODT because compositional fluctuations push the ODT to higher values of χN as $\overline{N}$ decreases. However, we do not have a precise measurement of the ODT in either case because we have never observed crystallization from an initially disordered state for these system sizes.[34,35] At best, we have previously established lower bounds for the ODT at $\chi N_{\rm ODT} \simeq 44.2$ for $\overline{N} = 3820$ and $\chi N_{\rm ODT} \simeq 63.7$ for $\overline{N} = 960$ from the melting of initially ordered systems.[35] Previous work indicates that micellar crystals can be only slightly undercooled,[42,43] suggesting that these lower bounds may be close to the true ODT.

This behavior of $\tau_{\rm s}$ shown in Figure 5 for BCC-forming systems is similar to that observed in related simulations of compositionally symmetric diblock copolymer melts,[38] but with

somewhat longer time scale. Simulations of lamellar-forming systems yields a value of $\tau_s/\tau_0 \approx 28$ near the ODT in simulations of the compositionally symmetric model S1-16, for which $\overline{N} = 239$. This is a model that is similar in most respects to the asymmetric model with $\overline{N} = 960$ considered here (asymmetric model S1-64), having a B-block of the same length (8 beads), while differing only in the length of the A block (8 beads for symmetric model S1-16 rather than 56 beads for the asymmetric model S1-64 studied here). Simulations of corresponding symmetric copolymers with chains of 32 beads (model S1-32) and $\overline{N} = 478$ gave $\tau_s/\tau_0 \approx 25$. Given the observed trends, we would expect a slightly smaller value of τ_s/τ_0 for a symmetric copolymer with $\overline{N} = 960$. The corresponding value for sphere-forming polymer with $\overline{N} = 960$ near our best estimate of its ODT is $\tau_s/\tau_0 \approx 100$. For an experimentally relevant value of $\overline{N} \sim 10^3$, the value of τ_s/τ_0 for a BCC-forming system with $f_B = 1/8$ is thus 4-5 times that of a symmetric polymer with the same value of $\overline{N}$. This difference is notable, but not as dramatic as we one might have thought in light of much more dramatic differences between lamellar- and sphere-forming systems in the rates of crystallization and rates of equilibration of q^* within the disordered phase.

Predicting Micelle Lifetime

Kim *et al.*[5] have showed that sphere-forming PI-PLA diblocks prepared by different routes can show different values of q^* that persist for surprisingly long times (at least 10^3 seconds) even in systems with much shorter rheological relaxation times (less than one second).[37] These authors hypothesized that q^* is controlled by the number concentration of micelles, and that persistence of non-equilibrium values of q^* in a liquid might be a result of the rarity of events that can create or destroy entire micelles.

In this section, we thus attempt to use the information obtained from our simulations to construct a theoretical estimate of the characteristic time scale for changes in the number of micelles in a micellar liquid. Changes in the number of micelles can occur either primarily by

stepwise growth processes, in which micelles are created by stepwise association of unimers and destroyed by stepwise dissociation, or by micelle fission and fusion. Early analyses of kinetics in micellar solutions[7–9,44] focused on the stepwise growth mechanism, and assumed negligible rates for micelle fission and fusion. A growing body of evidence from experiments and simulations has shown, however, that fission and fusion sometimes dominate, particularly in systems of very sparingly soluble surfactants.[13–15]

We cannot be certain which of these two competing mechanisms dominates in the simulation model considered here at conditions near the ODT. Comparison of parameters of the models considered here with those used in a previous simulation study of the mechanism of the slow process by Mysona *et al.*[13,14] suggests that a stepwise process is more likely. In that study, the authors compared estimated rates of stepwise association/dissociation processes to those of fission/fusion processes for micelles of AB asymmetric copolymers with 32 beads per chain, $f_{\mathrm{B}} = 1/8$ and $\overline{N} = 480$ dissolved in an A homopolymer solvent with the same total number of beads per chain as the copolymer, using simulation models similar to those considered here but with somewhat shorter chains. They found that stepwise processes appeared to dominate for more weakly segregated systems, with $\chi N_{\mathrm{B}} < 12$, while fission and fusion dominate for larger values of χN_{B}. The systems considered here have $\chi N < 70$ at the ODT, giving values of $\chi N_B < 9$ throughout the disordered phase. If we assume that processes that involve a single micelle (i.e., stepwise dissociation and fission) exhibit similar rates in a dense melt as those found for AB micelles dissolved in A homopolymer at similar values of χN_B, then the comparison suggests that stepwise processes are likely to dominate micelle birth and death within the disordered micellar state of the systems considered here.

In what follows, we consider a stepwise growth model to describe changes in the number of micelles in a dense micellar liquid. Specifically, we attempt to estimate the average time it would take an existing micelle to be destroyed by stepwise dissociation in the absence of fission and fusion, and denote this time τ_{d}. Analysis of a stepwise growth model provides an estimated upper bound for the true micelle lifetime, since we expect the overall lifetime

to be significantly less than this stepwise dissociation lifetime $\tau_{\rm d}$ if and only if fission and fusion actually dominate the slow process of interest.

Consider a micellar liquid with an equilibrium number concentration c_n for micellar clusters of aggregation number n, also known as "n-mers". In a system with well defined micelles, c_n has a maximum at some equilibrium aggregation number $n_{\rm e}$ and a minimum at a transition state value $n_{\rm t}$, such that $c_{n_{\rm e}} \gg c_{n_{\rm t}}$. This is the behavior observed for both of the models studied here at conditions near the ODT in our earlier work on equilibrium properties.[34,35] Let W_n denote a corresponding formation free energy, defined such that $c_n(\mathbf{r}) \propto e^{-W_n/k_{\rm B}T}$. The thermodynamic barrier to stepwise dissociation is given by the free energy

$$\Delta W_{\rm d} = W_{n_{\rm t}} - W_{n_{\rm e}} = k_{\rm B}T \ln(c_{n_{\rm e}}/c_{n_{\rm t}}) \tag{5}$$

required to "shrink" a micelle from the most probable value $n_{\rm e}$ to the transition state value $n_{\rm t}$ via a sequence of stepwise expulsion events. The distribution of cluster sizes required to compute this quantity is known for both models of interest from our previous work.[34,35]

We consider a stepwise growth model in which the aggregation number of each micelle changes via a Markov chain of insertion and expulsion events. Let r_n^- denote the rate for expulsion of any chain from an $(n+1)$-mer to create an n-mer. The corresponding rate r_n^+ for insertion of one chain into an n-mer is related to this expulsion rate by the principle of detailed balance, which requires that $r_n^- c_{n+1} = r_n^+ c_n$. For simplicity, and in the absence of data that would allow use of a more accurate treatment, we consider a model in which r_n^- is given by a constant r^- that is independent of n, which we approximate by

$$r^- = Q/\tau_{\rm ex} \quad , \tag{6}$$

where $\tau_{\rm ex}$ is the average time before any specific polymer in a micelle would be expelled, and Q is the average aggregation number.

The micelle dissociation lifetime $\tau_{\rm d}$ predicted by this model can be approximated in the

limit of a large dissociation barrier[13,14,44] as a product

$$\tau_{\rm d} \simeq \frac{2\pi\sigma_{\rm e}\sigma_{\rm t}}{r^-} \exp\left(\Delta W_d/k_{\rm B}T\right) \quad . \tag{7}$$

Here, $\sigma_{\rm e}$ is the width of the peak in c_n near the value $n = n_{\rm e}$ at which c_n is maximum, defined as a standard deviation, while $\sigma_{\rm t}$ is the corresponding width of the peak in $1/c_n$ vs. n near the transition state value $n = n_{\rm t}$ at which c_n is minimum.

Values for the quantities Q, $\exp(\Delta W_d/k_{\rm B}T)$, $\sigma_{\rm e}$ and $\sigma_{\rm t}$ can be obtained from an analysis of the equilibrium distribution of cluster sizes. Values for the fraction x_n of chains in clusters of aggregation number n, or n-mers, have been obtained in a previous study of equilibrium properties of the two models studied here.[35] These can be converted into estimates for the number concentration c_n of n-mers, for which $c_n v_c = x_n/n$, where v_c is the average volume per chain. The exponential factor is simply given by the ratio $\exp(\Delta W_d/k_{\rm B}T) = c_{n_{\rm e}}/c_{n_{\rm t}}$ of the local maximum and local minimum values of c_n. The average micelle aggregation number Q may be adequately approximated by the most probable aggregation number $n_{\rm e}$. Values of $\sigma_{\rm e}$ and $\sigma_{\rm t}$ have been estimated by fitting the behavior of c_n near $n_{\rm e}$ and the behavior of $1/c_n$ near $n_{\rm t}$ to a Gaussian distribution. An estimate of $\tau_{\rm d}$ may thus be obtained by equilibrium data with a measurement of the exchange time $\tau_{\rm ex}$.

For concreteness, we focus on the behavior of a system with $\overline{N} = 960$ at a value of $\chi N = 68.5$ near its estimated ODT. A plot of c_n vs. n for this system is given in SI, Fig. S4. For this system, we estimate $\tau_{\rm ex}/\tau_0 \simeq 90$, and examination of the cluster size distribution yields $\exp(\Delta W_d/k_{\rm B}T) = c_{n_{\rm e}}/c_{n_{\rm t}} \simeq 273$, $Q \simeq 100$, and $\sigma_{\rm e} \simeq 17$, $\sigma_{\rm t} \simeq 8$. Using these values in Eq. (7) yields an estimated micelle dissociation time

$$\tau_{\rm d}/\tau_0 \simeq 2 \times 10^5 \quad . \tag{8}$$

This estimate is more than 3 orders of magnitude greater than the structural relaxation time $\tau_{\rm s}/\tau_0 \simeq 100$ obtained for this system by examining the initial decay of $S(q^*, t)$.

Slowly evolving fluctuations of q^* that are related to slow changes in micelle number concentration might be expected to create a weak, very slowly decaying tail in both the intensity autocorrelation function and $S(q,t)$ at long times. The strength of the resulting feature might be expected to be particularly small, however, for q near the value q^* at which $S(q,t)$ is maximum, for which the change in intensity associated with a change in q^* would vanish to first order in an expansion in the change in q^*. In light of the limited length of our simulations, and of the large statistical fluctuations observed in our measurements of $S(q^*,t)$ near the ODT, we think it is unlikely that we would have been able to observe such a feature if it does exist, particularly if the time over which q^* fluctuates is indeed comparable to the value of $\tau_{\rm d}$ predicted above. We thus believe that our simulations do not rule out the possible existence of a very slow relaxation mechanism that would not be detectable in computationally feasible measurements of $S(q,t)$.

In previous work on equilibrium properties of the models considered here, an analysis of clusters formed in the melt showed that equilibrated melts exhibit frequent formation and destruction of very narrow, short-lived "bridges" or "throats" of core block material connecting neighboring micelles.[35] We have not, however, seen any evidence of irreversible fusion of small clusters into larger clusters via the formation these transient bridges. Instead, the bridges between micelles that we observed all appeared to break shortly after they were formed, rather than leading to formation of long-lived large clusters. We thus do not think that our previous observation of very short-lived bridges between micelles necessarily indicates that fission and fusion must dominate the slow process, or that these bridges represent an effective pathway for micelle fusion. Instead, as already noted, comparison with a previous simulation study of the slow process of copolymer micelles in a homopolymer matrix[13,13] instead indicates that stepwise processes are likely to dominate in the disordered phase at $\chi N \simeq (\chi N)_{\rm ODT}$.

The fact that the above estimate of $\tau_{\rm d}$ is much greater than the measured value of $\tau_{\rm s}$ establishes the plausibility of the physical picture proposed by Kim *et al.*,[5] in which the slow

relaxation of non-equilibrium values of q^* in disordered systems with $\overline{N} \sim 10^3$ near the ODT is controlled by very slow changes in micelle number concentration.

Any attempt to more quantitatively compare our simulation results to experiments would be complicated by the fact that different physical quantities have been measured in different studies, and by differences in values of f_B and $\overline{N}$ used in different studies. Specifically, comparison to analyses of experiments that compare scattering and rheology measurements[6] is complicated by the fact that we have not measured the stress relaxation modulus in these simulations. The simplest view of the relationship between scattering and rheology would be to assume that the terminal rheological relaxation time $\tau_{\rm tr}$ and the time $\tau_{\rm s}$ associated with the decay of $S(q^*, t)$ are both controlled in a liquid of long-lived micelles by a characteristic time scale for local structural re-arrangements, and that these two relaxation times should thus be similar. This picture is consistent both with the behavior of dense simple liquids, and with the results of simulations of lamellar diblock copolymers[38] in which both relaxation times were measured. This picture is not, however, compatible with the results of Patel *et al.*,[6] who instead obtained a structural relaxation time from XPCS experiments on melts of asymmetric diblock copolymers that exceeds $\tau_{\rm tr}$ by 1-2 orders of magnitude. We remain unsure of the physical reason for this observation by Patel *et al.*[6] We note, however, that if the terminal rheological relaxation time for the simulation model analyzed here actually is substantially less than the structural relaxation time $\tau_{\rm s}$ measured here, that would imply a value for the ratio $\tau_{\rm d}/\tau_{\rm tr}$ that is substantially larger than the value of the ratio $\tau_{\rm d}/\tau_{\rm s}$ that we attempt to predict here. Any such increase in the estimated value of $\tau_{\rm d}/\tau_{\rm tr}$ would thus bring our analysis of micelle lifetime into closer agreement with observations by Kim *et al.*,[5] which suggest the existence of an extremely large value $\tau_{\rm d}/\tau_{\rm tr}$ near the ODT.

Conclusions

Extensive molecular dynamics simulations have been used to quantify rates for several dynamical processes that occur in disordered melts of sphere-forming diblock copolymers near the ODT.

Measurements of tracer diffusivity shows a dependence on χN consistent with that seen in experiments. Nearly equal diffusivities are obtained in disordered and ordered phases at equal values of χN under conditions near the ODT for which both phases can be observed. Analysis of the relationship between diffusivity and rates of expulsion of polymers from micelles confirm that, near the ODT, diffusion occurs primarily by random hopping of polymers between neighboring micelles.

Structural relaxation has been probed by examining the decay of $S(q,t)$ for $q \simeq q^*$, which we use to define a structural relaxation time τ_s. For a model with a value of $\overline{N} \sim 10^3$ comparable to typical experimental values, the ratio of τ_s to the homopolymer Rouse relaxation time τ_0 reaches a value of $\tau_s/\tau_0 \sim 100$ near the ODT. This value of τ_s/τ_0 near the ODT is roughly 4 times greater than that observed in previous simulations of symmetric diblock copolymers with similar values of $\overline{N}$ near the disordered-lamellar transition. Symmetric and highly asymmetric copolymers thus both show a signficant decrease in rates of structural relaxation with increasing χN near the ODT. The relatively modest difference in the extent of this decrease, as characterized by the value of τ_s/τ_0, does not, however, appear to us to be sufficient to explain some of the dramatic reported differences in rates of crystallization and structural relaxation observed in lamellar and sphere-forming systems.

One of the most surprising experimental observation involving sphere-forming diblock copolymers is the observation by Kim *et al.*[5] of very long-lived differences in values of q^* in disordered phases that were created by melting different ordered structures. In an attempt to understand this, we used information from our simulations to estimate the micelle lifetime, using a simple model of stepwise micelle dissociation. When applied to a system with $\overline{N} \sim 10^3$, this model was found to predict a micelle lifetime near the ODT that is 3 orders of

magnitude greater than the relaxation time τ_s obtained from $S(q^*, t)$. This estimate provides support for the proposal of Kim *et al.*,[5] who hypothesized that the very slow relaxation of q^* observed near the ODT may be controlled by the rate of very slow changes in the number concentration of micelles.

Acknowledgement

This work was supported primarily by NSF grant DMR-1719692, using computational resources provided by the Minnesota Supercomputing Institute (MSI) at the University of Minnesota. Part of this work was carried out with equipment supported by funding from the National Science Foundation through the UMN MRSEC under Award Number DMR-2011401.

Supporting Information Available

Additional information on simulations; Mean-squared displacement data; Addition data for $n_L(t)$; Details for the dynamic structure factor calculation and additional data; Cluster size distribution data.

References

(1) Adams, J. L.; Quiram, D. J.; Graessley, W. W.; Register, R. A.; Marchand, G. R. Ordering Dynamics of Compositionally Asymmetric Styrene-Isoprene Block Copolymers. *Macromolecules* **1996**, *29*, 2929–2938, DOI: 10.1021/ma951261+.

(2) Cavicchi, K. A.; Lodge, T. P. Domain size equilibration in sphere-forming block copolymers. *J. Polym. Sci. B Polym. Phys.* **2003**, *41*, 715–724, DOI: 10.1002/polb.10427.

(3) Gillard, T. M.; Lee, S.; Bates, F. S. Dodecagonal Quasicrystalline Order in a Di-

block Copolymer Melt. *Proc. Natl. Acad. Sci. USA* **2016**, *113*, 5167–5172, DOI: 10.1073/pnas.1601692113.

(4) Kim, K.; Schulze, M. W.; Arora, A.; Lewis III, R. M.; Hillmyer, A.; Dorfman, K. D.; Bates, F. S. Thermal Processing of Diblock Copolymer Melts Mimics Metallurgy. *Science* **2017**, *356*, 520–523, DOI: 10.1126/science.aam7212.

(5) Kim, K.; Arora, A.; Lewis III, R.; Liu, M.; Li, W.; Shi, A.-C.; Dorfman, K.; Bates, F. Origins of low-symmetry phases in asymmetric diblock copolymer melts. *Proc. Natl. Acad. Sci. USA* **2018**, *115*, 847–854, DOI: 10.1073/pnas.1717850115.

(6) Patel, A. J.; Narayanan, S.; Sandy, A.; Mochrie, S. G. J.; Garetz, B. A.; Watanabe, H.; Balsara, N. P. Relationship between Structural and Stress Relaxation in a Block-Copolymer Melt. *Phys. Rev. Lett.* **2006**, *96*, 257801, DOI: 10.1103/PhysRevLett.96.257801.

(7) Aniansson, E. A.; Wall, S. N. On the kinetics of step-wise micelle association. *J. Phys. Chem.* **1974**, *78*, 1024–1030, DOI: 10.1021/j100603a016.

(8) Aniansson, E. A.; Wall, S. N.; M., A.; Hoffmann, H.; Kielmann, I.; W., U.; Zana, R.; Lang, J.; Tondre, C. Theory of the kinetics of micelle equilibria and quantitative interpretation of chemical relaxation studies of micellar solutions of ionic surfactants. *J. Phys. Chem.* **1976**, *80*, 905–922, DOI: 10.1021/j100550a001.

(9) Halperin, A.; Alexander, S. Polymeric Micelles: Their Relaxation Kinetics. *Macromolecules* **1989**, *22*, 2403–2412, DOI: 10.1021/ma00195a069.

(10) Dormidontova, E. E. Micellization kinetics in block copolymer solutions: Scaling model. *Macromolecules* **1999**, *32*, 7630–7644, DOI: 10.1021/ma9809029.

(11) Halperin, A. On micellar exchange: The role of the insertion penalty. *Macromolecules* **2011**, *44*, 5072–5074, DOI: 10.1021/ma200811x.

(12) Nyrkova, I. A.; Semenov, A. N. On the theory of micellization kinetics. *Macromol. Theory Simul.* **2005**, *14*, 569–585, DOI: 10.1002/mats.200500010.

(13) Mysona, J. A.; McCormick, A. V.; Morse, D. C. Mechanism of Micelle Birth and Death. *Phys. Rev. Lett.* **2019**, *123*, 038003, DOI: 10.1103/PhysRevLett.123.038003.

(14) Mysona, J. A.; McCormick, A. V.; Morse, D. C. Simulation of Diblock Copolymer Surfactants. II. Micelle Kinetics. *Phys. Rev. E* **2019**, *100*, 012603, DOI: 10.1103/PhysRevE.100.012603.

(15) Lodge, T. P.; Seitzinger, C. L.; Seeger, S. C.; Yang, S.; Gupta, S.; Dorfman, K. D. Dynamics and equilibration mechanisms in block copolymer particles. *ACS Polymers Au* **2022**, *2*, 397–416, DOI: 10.1021/acspolymersau.2c00033.

(16) Yokoyama, H.; Kramer, E. J. Self-Diffusion of Asymmetric Diblock Copolymers with a Spherical Domain Structure. *Macromolecules* **1998**, *31*, 7871–7876, DOI: 10.1021/ma9805250.

(17) Yokoyama, H.; Kramer, E. J.; Fredrickson, G. H. Simulation of Diffusion of Asymmetric Diblock and Triblock Copolymers in a Spherical Domain Structure. *Macromolecules* **2000**, *33*, 2249–2257, DOI: 10.1021/ma991203e.

(18) Cavicchi, K. A.; Lodge, T. P. Self-Diffusion and Tracer Diffusion in Sphere-Forming Block Copolymers. *Macromolecules* **2003**, *36*, 7158–7164, DOI: 10.1021/ma0346815.

(19) Pedemonte, E.; Turturro, A.; Bianchi, U.; Devetta, P. The cubic structure of a SIS three block copolymer. *Polymer* **1973**, *14*, 145–150, DOI: 10.1016/0032-3861(73)90107-9.

(20) Huang, Y. Y.; Hsu, J. Y.; Chen, H. L.; Hashimoto, T. Existence of fcc-packed spherical micelles in diblock copolymer melt. *Macromolecules* **2007**, *40*, 406–409, DOI: 10.1021/ma062149m.

(21) Hsu, N. W.; Nouri, B.; Chen, L. T.; Chen, H. L. Hexagonal Close-Packed Sphere Phase of Conformationally Symmetric Block Copolymer. *Macromolecules* **2020**, *53*, 9665–9675, DOI: 10.1021/acs.macromol.0c01445.

(22) Zhang, C.; Vigil, D. L.; Sun, D.; Bates, M. W.; Loman, T.; Murphy, E. A.; Barbon, S. M.; Song, J.-a.; Yu, B.; Fredrickson, G. H.; Whittaker, A. K.; Hawker, C. J.; Bates, C. M. Emergence of Hexagonally Close-Packed Spheres in Linear Block Copolymer Melts. *J. Am. Chem. Soc.* **2021**, *143*, 14106–14114, DOI: 10.1021/jacs.1c03647.

(23) Dorfman, K. D. Frank–Kasper Phases in Block Polymers. *Macromolecules* **2021**, *54*, 10251–10270, DOI: 10.1021/acs.macromol.1c01650.

(24) Papadakis, C. M.; Almdal, K.; Mortensen, K.; Vigild, M. E.; Štěánek, P. Unexpected phase behavior of an asymmetric diblock copolymer. *J. Chem. Phys.* **1999**, *111*, 4319–4326, DOI: 10.1063/1.479730.

(25) Grason, G. M.; DiDonna, B. A.; Kamien, R. D. Geometric Theory of Diblock Copolymer Phases. *Phys. Rev. Lett.* **2003**, *91*, 058304, DOI: 10.1103/PhysRevLett.91.058304.

(26) Lee, S.; Bluemle, M. J.; Bates, F. S. Discovery of a Frank–Kasper σ phase in sphere-forming block copolymer melts. *Science* **2010**, *330*, 349–353, DOI: 10.1126/science.1195552.

(27) Xie, N.; Li, W.; Qiu, F.; Shi, A.-C. σ phase formed in conformationally asymmetric AB-type block copolymers. *ACS Macro Lett.* **2014**, *3*, 906–910, DOI: 10.1021/mz500445v.

(28) Bates, M. W.; Lequieu, J.; Barbon, S. M.; Lewis III, R. M.; Delaney, K. T.; Anastasaki, A.; Hawker, C. J.; Fredrickson, G. H.; Bates, C. M. Stability of the A15 phase in diblock copolymer melts. *Proc. Natl. Acad. Sci. USA* **2019**, *116*, 13194–13199, DOI: 10.1021/ma801268d.

(29) Jeon, S.; Jun, T.; Jo, S.; Ahn, H.; Lee, S.; Lee, B.; Ryu, D. Y. Frank–Kasper Phases Identified in PDMS-b-PTFEA Copolymers with High Conformational Asymmetry. *Macromol. Rapid Commun.* **2019**, *40*, 1900259, DOI: 10.1002/marc.201900259.

(30) Schwab, M.; Stühn, B. Thermotropic Transition from a State of Liquid Order to a Macrolattice in Asymmetric Diblock Copolymers. *Phys. Rev. Lett.* **1996**, *76*, 924–927, DOI: 10.1103/PhysRevLett.76.924.

(31) Wang, J.; Wang, Z. G.; Yang, Y. Nature of disordered micelles in sphere-forming block copolymer melts. *Macromolecules* **2005**, *38*, 1979–1988, DOI: 10.1021/ma047990j.

(32) Fredrickson, G. H.; Helfand, E. Fluctuation effects in the theory of microphase separation in block copolymers. *J. Chem. Phys.* **1987**, *87*, 697–705, DOI: 10.1063/1.453566.

(33) Dormidontova, E. E.; Lodge, T. P. The order-disorder transition and the disordered micelle regime in sphere-forming block copolymer melts. *Macromolecules* **2001**, *34*, 9143–9155, DOI: 10.1021/ma010098h.

(34) Chawla, A.; Bates, F. S.; Dorfman, K. D.; Morse, D. C. Identifying a critical micelle temperature in simulations of disordered asymmetric diblock copolymer melts. *Phys. Rev. Mater.* **2021**, *5*, L092601, DOI: 10.1103/PhysRevMaterials.5.L092601.

(35) Chawla, A.; Bates, F. S.; Dorfman, K. D.; Morse, D. C. Simulations of sphere-forming diblock copolymer melts. *Phys. Rev. Mater.* **2022**, *6*, 095602, DOI: 10.1103/PhysRevMaterials.6.095602.

(36) Glaser, J.; Medapuram, P.; Beardsley, T. M.; Matsen, M. W.; Morse, D. C. Universality of block copolymer melts. *Phys. Rev. Lett.* **2014**, *113*, 068302, DOI: 10.1103/PhysRevLett.113.068302.

(37) Lee, S.; Leighton, C.; Bates, F. S. Sphericity and Symmetry Breaking in the Formation

of Frank–Kasper Phases from One Component Materials. *Proc. Natl. Acad. Sci. USA* **2014**, *111*, 17723–17731, DOI: 10.1073/pnas.1408678111.

(38) Ghasimakbari, T.; Morse, D. C. Dynamics and Viscoelasticity of Disordered Melts of Symmetric Diblock Copolymers. *Macromolecules* **2019**, *52*, 7762–7778, DOI: 10.1021/acs.macromol.9b01287.

(39) Fredrickson, G. H.; Larson, R. G. Viscoelasticity of homogeneous polymer melts near a critical point. *J. Chem. Phys.* **1987**, *86*, 1553–1560, DOI: 10.1063/1.452194.

(40) Medapuram, P.; Glaser, J.; Morse, D. C. Universal Phenomenology of Symmetric Diblock Copolymers near the Order-Disorder Transition. *Macromolecules* **2015**, *48*, 819–839, DOI: 10.1021/ma5017264.

(41) Semenov, A. N.; Anastasiadis, S. H.; Boudenne, N.; Fytas, G.; Xenidou, M.; Hadjichristidis, N. Dynamic Structure Factor of Diblock Copolymers in the Ordering Regime. *Macromolecules* **1997**, *30*, 6280–6294, DOI: 10.1021/ma970700x.

(42) Beardsley, T. M.; Matsen, M. W. Fluctuation Correction for the Order – Disorder Transition of Diblock Copolymer Melts. *J. Chem. Phys.* **2021**, *154*, 124902, DOI: 10.1063/5.0046167.

(43) Cheong, G. K.; Dorfman, K. D. Disordered Micelle Regime in a Conformationally Asymmetric Diblock Copolymer Melt. *Macromolecules* **2021**, *54*, 9868–9878, DOI: 10.1021/acs.macromol.1c01629.

(44) Kahlweit, M.; Teubner, M. On the kinetics of micellization in aqueous solutions. *J. Phys. Chem.* **1980**, *13*, 1–64, DOI: 10.1016/0001-8686(80)87001-1.

TOC Graphic

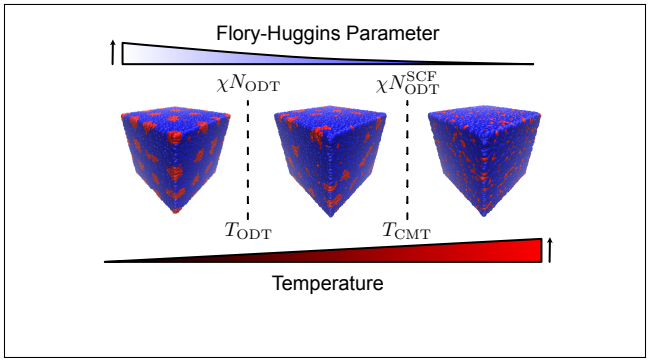
Flory-Huggins Parameter
χN_{ODT}
$\chi N_{\mathrm{ODT}}^{\mathrm{SCF}}$
T_{ODT}
T_{CMT}
Temperature

Supporting Information for "Chain and Structural Dynamics in Melts of Sphere-Forming Diblock Copolymers"

Anshul Chawla, Frank S. Bates, Kevin D. Dorfman,* and David C. Morse†

Department of Chemical Engineering and Materials Science,

University of Minnesota – Twin Cities,

421 Washington Ave. SE, Minneapolis, MN 55455, USA

I. METHODS

The methodology used here follows closely from our previous work [1, 2]. Briefly, we have leveraged two existing models for diblock copolymer melts, referred to as S1-64 and S2-64 in Ref. 3. In the simulation presented here, each chain contains 64 beads, with 56 A beads with 8 B beads, giving a minority block volume fraction $f_{\mathrm{B}} = 1/8$. Consecutive beads are connected by harmonic bonds with a bond potential

$$V_{\mathrm{bond}}(r) = \frac{\kappa}{2} r^2 \tag{S-1}$$

with spring constant κ. All pairs of beads of monomer types i and j interact via a non-bonded potential of the form

$$V_{ij}(r) = \frac{\epsilon_{ij}}{2}\left(1 - \frac{r}{\sigma}\right)^2 \tag{S-2}$$

for r less than a cutoff length σ, and $V_{ij}(r) = 0$ for $r > \sigma$. The parameter ϵ_{ij} governs the repulsion between beads of type i and j, with $\epsilon_{\mathrm{AA}} = \epsilon_{\mathrm{BB}} = 25 k_{\mathrm{B}} T$, where k_{B} is Boltzmann's constant and T is the absolute temperature. The parameter

$$\alpha = \frac{\epsilon_{\mathrm{AB}} - \epsilon_{\mathrm{AA}}}{k_{\mathrm{B}} T} \tag{S-3}$$

controls the tendency to phase separate. For models S1 and S2, values of the spring constant κ and pressure P in constant pressure simulations have been tuned in Ref. 3 to produce invariant degrees of polymerization $\bar{N} = 960$ (for model S1) and $\bar{N} = 3820$ (for model S2). Moreover, the relationship between the input parameter α and the effective Flory-Huggins parameter χ has been determined for these models fitting the structure of the disordered state to the renormalized one-loop theory [3, 4]. As a result, we are able to leverage the parameters of Ref. 3 to produce simulation data at two different values of $\bar{N}$, and plot results as functions of χN.

Simulations were performed in the NPT ensemble using a Martyna-Tuckerman-Tobias-Klein barostat-thermostat [5, 6] using HOOMD-blue [7, 8]. The number of chains in each system were selected to match, as closely as possible, the preferred number to create a $3 \times 3 \times 3$ BCC system, following the detailed discussion in the supporting information of our prior work [1, 2]. To study dynamics of the ordered state, a guiding field was applied to

* dorfman@umn.edu
† morse012@umn.edu

promote chain aggregation into micelles at the BCC lattice positions. The guiding field was only used to create an ordered initial state, and then removed. The system sizes, α values, number of molecules, and the number of time steps for each simulation are reported in the Supplementary Material of Ref. 2.

To determine the exchange time for a micelle, we first identified isolated micelles using the cluster identification algorithm reported in our prior work [1]. Then, using the positions of these micelle singlets, we map micelles from a sampled configuration at time t to a configuration at a time $t + \Delta t$ and count the number of chains $n_L(t)$ that were retained. If fluctuations in the micelle position relative to its BCC lattice site results in collision with a neighboring micelle to form a multiplet at time interval Δt, that micelle is discarded from the analysis. Throughout this analysis, we keep track of the number $n_L(t)$ of labelled chains retained within the micelle after a specified time interval t, and average this quantity over all micelle singlets and all initial times.

II. POLYMER MEAN-SQUARED DISPLACEMENTS

Figure S-1 shows examples of results for mean-squared displacement $g(t)$ of the polymer center of mass vs. time for simulations with both values of $\overline{N}$ considered in this work.

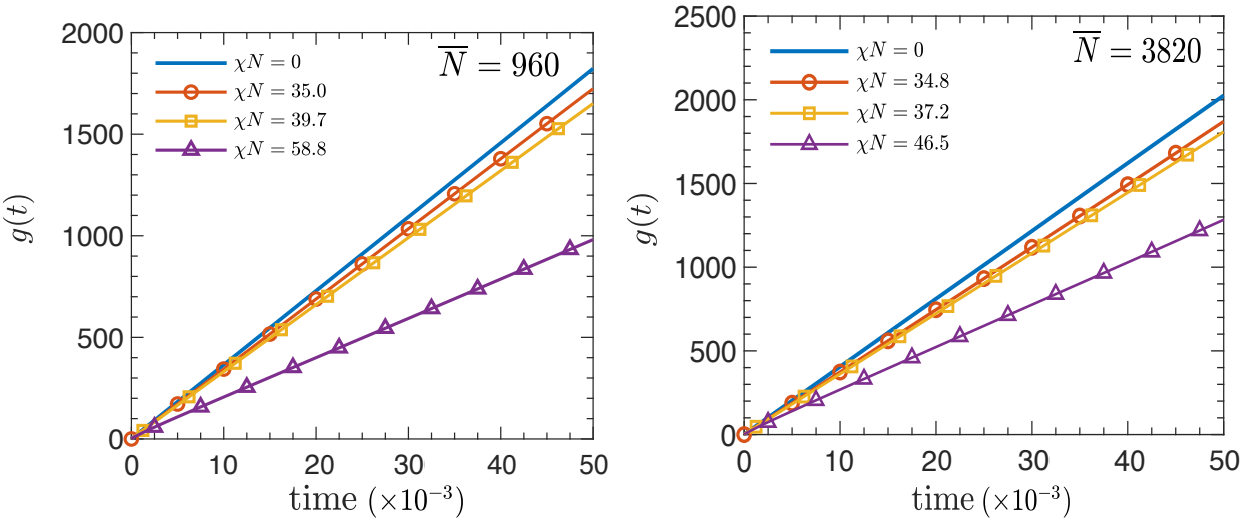

FIG. S-1. Mean-squared displacement $g(t)$ vs. time t for simulations having $\overline{N} = 960$ (left) and $\overline{N} = 3820$ (right). Values for $g(t)$ and time t in these plots are shown in simulation units of length and time in which the range of interaction σ, the thermal energy $k_{\rm B}T$ and the monomer or bead mass $m_{\rm b}$ are all taken to unity, i.e., in which $\sigma = k_{\rm B}T = m_{\rm b} = 1$. The corresponding unit of time is $\sigma\sqrt{m_{\rm b}/k_{\rm B}T}$.

III. CHAIN EXCHANGE

Figure S-2 shows examples of results for the number $n_L(t)$ of chains that are in a micelle at time $t = 0$ that remain in the same micelle after time t, from simulations of the ordered phase of systems with $\overline{N} = 3820$. The dashed lines in the plot are the fits to an exponential decay

$$n_L(t) = Q \exp\left(-t/\tau_{\rm ex}\right) + c$$

from which we have extracted values for $\tau_{\rm ex}$ for each value of χN. Analogous data for systems with $\overline{N} = 960$ are shown in the inset of Fig. 3 of the main text.

IV. DYNAMIC STRUCTURE FACTOR

To obtain the dynamic structure factor, we define the composition field $\psi(\mathbf{r}, t)$ at a position $\mathbf{r}$ and time t as

$$\psi(\mathbf{r}, t) = \frac{c_A(\mathbf{r}, t) - c_B(\mathbf{r}, t)}{2} \quad , \tag{S-4}$$

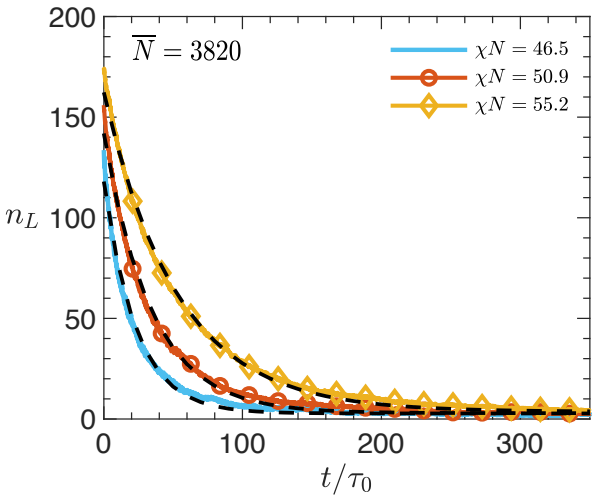

FIG. S-2. Number of labeled chains $n_L(t)$ retained in a micelle vs. the normalized time delay t/τ_0, in the ordered phase of systems with $\overline{N} = 3820$. The dashed lines show fits to an exponential decay.

where $c_i(\mathbf{r}, t)$ is the instantaneous concentration of particle type i. The Fourier transform of this concentration field can be expressed as

$$\hat{\psi}(\mathbf{q}, t) = \int d^3\mathbf{r}\, e^{-i\mathbf{q}\cdot\mathbf{r}} \psi(\mathbf{r}, t) \tag{S-5}$$

and can therefore be calculated as

$$\hat{\psi}(\mathbf{q}, t) = \frac{1}{2} \sum_j e^{-i\mathbf{q}\cdot\mathbf{r_j}} \epsilon_j \quad , \tag{S-6}$$

where j is a particle index, $\mathbf{r_j}$ is the position of particle j and ϵ_j is $+1$ for particle type A and -1 for type B.

The dynamic structure factor $S(\mathbf{q}, t)$ is then defined as the autocorrelation function of $\hat{\psi}(\mathbf{q}, t)$,

$$S(\mathbf{q}, t) = \frac{1}{V} \langle \hat{\psi}^*(\mathbf{q}, t) \hat{\psi}(\mathbf{q}, 0) \rangle \quad , \tag{S-7}$$

where V is the volume of the simulation box and $\hat{\psi}^*$ is the complex conjugate of $\hat{\psi}$. For a disordered phase, where there is no preferred direction, $S(\mathbf{q}, t)$ should be a function of the scalar wavenumber $q = |\mathbf{q}|$ and time t. The static structure factor of the melt can be directly be obtained from equation S-7 by setting $t = 0$.

The structural relaxation time for a given wavenumber q is then calculated by fitting the initial decay of the autocorrelation function $S(q, t)$ to an exponential function. It has been

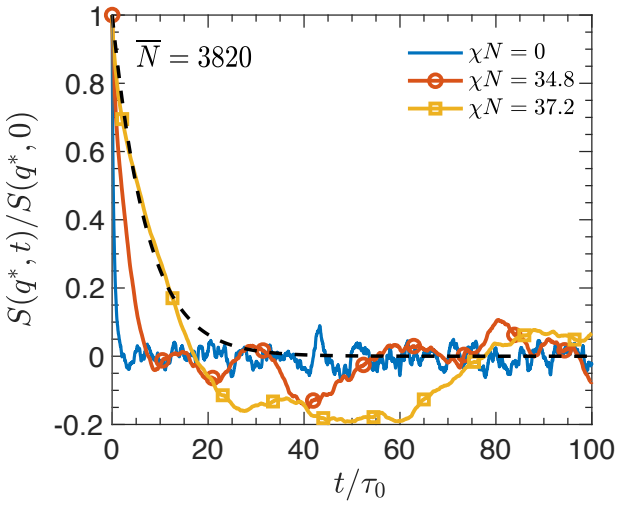

FIG. S-3. Normalized dynamical structure factor $S(q^*, t)/S(q^*, 0)$ at the peak wavenumber q^* *vs.* normalized time t/τ_0, where τ_0 is the homopolymer Rouse relaxation time, for simulations having $\overline{N} = 3820$ and three different values of χN. Circle ($\chi N = 34.8$) and square ($\chi N = 37.2$) markers are used to help distinguish different curves, but are not shown every data point: circles are shown every 2000 data points and squares are shown every 1000 data points. The black dashed line is an example of exponential fit to the initial decay shown for $\chi N = 37.2$.

shown that the maximum structural relaxation time or the terminal structural relaxation time τ_s corresponds to the value extracted from the dynamical structure factor $S(q^*, t)$ where q^* is the peak wavenumber [9].

Figure S-3 shows the decay in the normalized dynamical structure factor $S(q^*, t)/S(q^*, 0)$ with respect to the normalized time t/τ_0 at different values of χN for simulations having $\bar{N} = 3820$. Similar data for $\bar{N} = 960$ appear in the main text.

V. CLUSTER SIZE DISTRIBUTION

Figure S-4 shows the normalized number concentration c_n of clusters of aggregation number n for $\chi N = 68.5$ and $\overline{N} = 960$ that was used in the estimate of micelle dissociation lifetime presented in the main text.

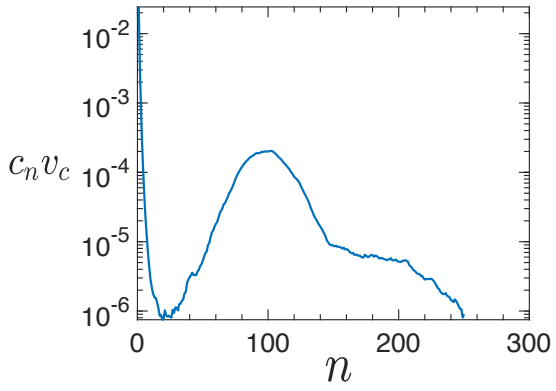

FIG. S-4. Normalized concentration of clusters $c_n v_c$ of aggregation number n *vs.* n for $\chi N = 68.5$ and $\overline{N} = 960$. Here c_n is the number concenteration of micelles and v_c is the average volume per chain.

[1] A. Chawla, F. S. Bates, K. D. Dorfman, and D. C. Morse, Identifying a critical micelle temperature in simulations of disordered asymmetric diblock copolymer melts, Phys. Rev. Mater. **5**, L092601 (2021).

[2] A. Chawla, F. S. Bates, K. D. Dorfman, and D. C. Morse, Simulations of sphere-forming diblock copolymer melts, Phys. Rev. Mater. **6**, 095602 (2022).

[3] P. Medapuram, J. Glaser, and D. C. Morse, Universal phenomenology of symmetric diblock copolymers near the order-disorder transition, Macromolecules **48**, 819 (2015).

[4] J. Glaser, J. Qin, P. Medapuram, and D. C. Morse, Collective and single-chain correlations in disordered melts of symmetric diblock copolymers: Quantitative comparison of simulations and theory, Macromolecules **47**, 851 (2014).

[5] G. J. Martyna, D. J. Tobias, and M. L. Klein, Constant pressure molecular dynamics algorithms, J. Chem. Phys. **101**, 4177 (1994).

[6] G. J. Martyna, M. E. Tuckerman, D. J. Tobias, and M. L. Klein, Explicit reversible integrators for extended systems dynamics, Mol. Phys. **87**, 1117 (1996).

[7] J. A. Anderson, C. D. Lorenz, and A. Travesset, General purpose molecular dynamics simulations fully implemented on graphics processing units, J. Comput. Phys. **227**, 5342 (2008).

[8] J. Glaser, T. D. Nguyen, J. A. Anderson, P. Lui, F. Spiga, J. A. Millan, D. C. Morse, and S. C. Glotzer, Strong scaling of general-purpose molecular dynamics simulations on GPUs, Comput. Phys. Commun. **192**, 97 (2015).

[9] A. N. Semenov, S. H. Anastasiadis, N. Boudenne, G. Fytas, M. Xenidou, and N. Hadjichristidis, Dynamic structure factor of diblock copolymers in the ordering regime, Macromolecules **30**, 6280 (1997), https://doi.org/10.1021/ma970700x.